Building and Environment 262 (2024) 111828

Contents lists available at ScienceDirect

Building and Environment

journal homepage: www.elsevier.com/locate/buildenv

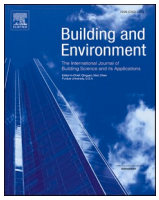

Investigation of a DNA tagged aerosol tracer method for In Situ evaluation of germicidal UV air cleaner effectiveness

Ilan Arvelo [a,*], Ernest R. Blatchley III [b], William P. Bahnfleth [c], Phil Arnold [a], Ashley Fry [a], Maria Topete [d], Ling Zhou [d], William Palmer [e], Patrick J. Piper [f], Jianping Zhang [d], W. Andrew Dexter [g], Nilson Palma [a], Nicholas J. Heredia [a]

[a] SafeTraces Inc., United States
[b] Purdue University, United States
[c] The Pennsylvania State University, United States
[d] Bolb Inc., United States
[e] AeroMed Inc., United States
[f] Far UV Technologies Inc., United States
[g] Aerosol Research and Engineering Laboratories Inc., United States

ARTICLE INFO

Keywords:
UV air disinfection measurement
Airborne pathogen surrogate
DNA aerosol tracer
Indoor air quality
Equivalent clean air

ABSTRACT

Transmission of respiratory pathogens occurs primarily in indoor settings, interventions to reduce the risk of their transmission include increases in outdoor air introduction, filtration, and ultraviolet germicidal irradiation (UVGI). However, validating these interventions is challenging, particularly in actual applications. This study introduces an aerosol tracer system utilizing DNA as tracer molecule, aimed at quantitative characterization of the performance of indoor air cleaning systems. Two DNA tracers, designed one to be relatively UV-resistant and another relatively UV-sensitive, were employed to assess air quality changes related to filtration and ventilation and the contributions of UVGI fixtures in various built environments. We conducted controlled UV exposure experiments of DNA-tagged tracers on foil coupons, aerosolization studies in a test chamber, and in a commercial building conference room. The DNA tracer results provided insights at the point of sampling into the effects of complex airflow dynamics. Additionally, a way to scale the DNA tracer results to MS2 bacteriophage is proposed. Four distinct UV devices challenged with MS2 in a chamber test produced equivalent clean airflow rates of 13–147 CFM. Scaled equivalent clean airflow rates in a commercial building setting using the UV-sensitive tracer varied from 47 percent less to 101 percent more than the chamber results, possibly due to differences in airflow patterns, equipment configuration, and other factors. Our findings provide quantitative understanding of the interaction between UV-sensitive aerosols and the built environment, with implications for environmental monitoring, measuring UVGI fixture impact in field settings, and addressing current technologies limitations for assessing UVGI disinfection efficacy.

1. Introduction

Airborne exposure to pathogens, including viruses like coronaviruses (responsible for COVID-19 and some common cold strains), influenza, measles, respiratory syncytial virus (RSV), Human metapneumovirus (HMPV), and bacteria such as *M. tuberculosis*, is a significant factor in the transmission of the infectious diseases they cause [1]. Mitigating the airborne spread of these pathogens is crucial for public health. Interventions such as increased air exchange, filtration, and ultraviolet germicidal irradiation (UVGI) aim to reduce the concentration of viable pathogens in the air, hence, reducing the risk of infection by reducing inhalational exposure [2]. Among these interventions, UVGI systems hold great promise for effective pathogen control, offering both significant efficacy and cost-effectiveness in terms of capital and operating expenses [3].

The effectiveness of an intervention may vary across different settings. Designing and optimizing such systems necessitates a comprehensive approach that combines numerical simulations and empirical

* Corresponding author./
E-mail addresses: ilan@safetraces.com, arveloy@gmail.com (I. Arvelo).

https://doi.org/10.1016/j.buildenv.2024.111828
Received 23 February 2024; Received in revised form 14 June 2024; Accepted 8 July 2024
Available online 9 July 2024

testing. For example, an air cleaning system for a hospital might greatly benefit from design and optimization, whereas for non-critical environments such as a residential setting, such modeling and optimization would be impractical and cost prohibitive [4]. Numerical simulations, such as Computational Fluid Dynamics (CFD) and fluence rate field models (e.g., ray tracing), provide insights into the potential distribution and impact of UVGI within enclosed spaces. While CFD was not employed in the current study, it is worth noting that CFD is commonly used to simulate indoor air quality (IAQ) dynamics in the built environment, although its broad application in commercial building settings can be challenging [5,6].

Empirical testing, on the other hand, involves experiments using non-pathogenic challenge agents to quantify inactivation or physical separation under various operating conditions. Conventionally, such tests have been conducted in specialized environments like IAQ chambers. However, a critical challenge arises in translating test results from controlled environments to commercial building application settings. Currently, there is no method that combines mimicking the particle size distribution of a human upper respiratory aerosol emission that can be used for onsite testing of UVGI system efficacy, highlighting the need to develop robust new test methods and associated analyses.

An important limitation on effective application of the current methods for reducing human exposure to airborne pathogens in public spaces is the lack of a safe, single indicator that can represent the effectiveness of air purification devices, while taking into account the multiple mechanisms that affect the pathogen decay rate. Given the inability to assess installed effectiveness, it is often difficult to justify the cost of air filtration and cleaning devices, such as filters or UVGI fixtures.

Respiratory aerosols can be generated from alveolar, bronchiolar, bronchial, laryngeal, and oral fluids [7,8]. Airborne pathogens from human emissions are released in these fluids, then they desiccate to a fraction of their initial size [9], depending on initial particle size and environmental conditions. Their concentration in air will diminish by gravitational deposition, natural inactivation, removal by filters, dilution by the introduction of clean outside air, inactivation by exposure to UV radiation, and other causes.

This study evaluates a test method based on a UV-sensitive aerosol tracer that utilizes DNA as a tracer molecule subject to similar decay mechanisms as other airborne pathogens from a human emission, in order to address the lack of practical aerosol test methodologies. Nucleic acids, such as DNA, are ideal model substrates because they are one of the major components of viruses and bacteria that are susceptible to damage by UV wavelengths, which contributes to their germicidal inactivation [10]. The DNA-tagged liquid released in aerosol form is quantifiable and its concentration is sensitive to deposition, filtration, dilution, and UVGI exposure. Harding et al., 2016 introduced the use of DNA for tracking aerosol movement. One of the main advantages noted in their study was the ability to distinguish tagged particles from background aerosol concentration (given that the DNA sequences used are not naturally present in the air), and that the DNA can be carried in food additives generally recognized as safe [11]. DNA-based aerosol tracers are commonly used to assess ventilation and filtration of HVAC systems in the built environment [12], however until now they have not been used to measure the impact of UVGI fixtures.

Our study utilized a DNA tracer system comprising UV-resistant (Tag-D1) and UV-sensitive (Tag-LM4) sequences, designed to measure physical removal effects separately from UV-C radiation exposure. By employing controlled UV exposure experiments and conducting aerosolization studies in commercial buildings, we aimed to provide empirical data linking DNA-tagged aerosols to bacteriophage aerosol UV response, shedding light on the intricate dynamics of UV-sensitive aerosols indoors. This multidimensional approach contributes to the broader discussion of optimizing IAQ and safety, acknowledging the diverse settings and the need for context-specific solutions. The system, utilizing short DNA molecules as tracer molecules and analyzed via droplet digital polymerase chain reaction (ddPCR), offers a promising means of quantifying DNA-tagged aerosols on air filters and assessing their removal by ventilation, with the inclusion of a UV-sensitive tag facilitating quantification of UV-C exposure. Our focus was on the development and deployment of UV-sensitive aerosol technology, particularly in understanding the interaction between airflow dynamics and UV-C fluence rate fields within environments equipped with UVGI fixtures. Differential analysis between the UV-resistant and UV-sensitive tracers allows assessment of the impact of UVGI fixtures on the local environment, aiding in estimating aerosol-associated pathogen inactivation achieved through UVGI deployment. This method provides a means to quantify physical separation effects by filtration or air exchange, as well as pathogen inactivation resulting from UV-C exposure, and can be applied directly in occupied settings, eliminating the need for translation from test to application environments.

The objectives of this study were to demonstrate the possibility of using selected DNA sequences as indicators of UV-C exposure by means of their decay rate in surfaces and aerosol form. Furthermore, we aimed to correlate DNA reduction rate due to UV-C exposure with a pathogen surrogate microorganism, such as bacteriophage MS2, in aerosol form inside a controlled test environment. Lastly, show the DNA indicator's applicability in a commercial setting as a way to assess the effectiveness of different UVGI systems used for pathogen control.

2. Materials and methods

2.1. DNA-tagged liquid suspension preparation

The DNA-Tag tracer solutions were formulated with 99 % water and 1 % solids, composed of DNA and proprietary, non-toxic components that are generally regarded as safe (GRAS) by the FDA. The DNA oligonucleotides, purchased from IDT (Integrated DNA Technologies, Coralville, IA), were custom sequences of fewer than 200 base pairs each. The UV-sensitive tag sequence underwent prior optimization for its response to UV radiation emitted by an ESCO CRF UV-30 A low-pressure mercury arc lamp (nearly monochromatic emission at a characteristic wavelength of 254 nm).

The UV-sensitive tracer was designed to incorporate UV-sensitive DNA sequence motifs known to produce photolesions upon UV exposure, such as "pyrimidine dimers, cyclobutane pyrimidine dimers (CPDs) and pyrimidine-pyrimidone (6–4) photoproducts [(6–4)PPs] between adjacent bases in DNA" [13,14]. Such DNA damage inhibits the replication of the UV-exposed DNA during amplification in a PCR reaction [15]. This results in a signal reduction from the UV-exposed DNA that can be measured from fluorescence signal generated in a TaqMan assay that targets the DNA molecules. The UV-resistant tag was designed to exclude thymine dimers and sequences prone to CPDs. The DNA-tags have been qualified to be stable under ambient office lighting conditions and have a shelf life of at least nine months.

Proprietary sequences of the DNA molecules used as tracers were inspired by naturally occurring sequences that would not be found in the test environment, as well as published literature on UV effects on DNA sequences [16]. The concentration of DNA in the tag solution was approximately 4,875,000,000 copies per μL for the UV-sensitive tag and 3,700,000,000 copies per μL for the UV-insensitive tag, as determined by TaqMan assays via ddPCR (QX200 system, Bio-Rad Laboratories) after extraction from coupons with an extraction buffer (see below methodology).

2.2. DNA-tag sensitivity to UV radiation on surfaces

Coupons were created by applying 50 μL of the tag solution to foil coupons (PCR plate heat seals, Bio-Rad Laboratories, Hercules, CA part number 1814040), air-drying them, and subsequently exposing them to a controlled range of UV-C doses. Rectangular foil coupons (dimensions: 6.98 cm by 8.26 cm) were used for exposure of the DNA tags to UV-C radiation. A circle (diameter = 5.08 cm) was drawn on each coupon

and 50 μL of tag solution was spotted and air-dried within the circle. Foil coupon UV-C exposures were conducted under collimated beams [17] that were built around the UV-C sources described in Table 1.

The optically-filtered KrCl lamp emits peak irradiance at 222 nm, with a full width at half maximum (FWHM) bandwidth of roughly 2 nm. The low-pressure Hg lamp is essentially monochromatic at 254 nm, with a FWHM bandwidth of less than 1 nm. The UV LEDs used in this experiment have an emission peak at about 282 nm, with a FWHM bandwidth of roughly 10 nm (see Fig. S1 for relative output spectra of UV sources used). All three sources have minor emission lines at longer wavelengths. The optically-filtered KrCl excimer lamp, and the low-pressure Hg lamp produce very little ozone. Nonetheless, to prevent any potential exposure to generated ozone from the lamps, the experiments were performed in a hood and the air flow pattern in the hood, together with the geometry and construction of the collimator (as well as the very modest ozone production rate) dictate that any exposure to ozone would be attributable to ozone naturally present.

For each UV source type, exposures were controlled to achieve delivered UV doses of 10, 20, 30, 50, and 100 mJ/cm^2. Triplicate exposures were conducted for each dose. Exposure times required to deliver these target doses were calculated based on measured values of incident irradiance at the horizontal planar surface located below the end of each collimated beam where samples were exposed. Incident irradiance at these locations was measured for each collimated UV source using a radiometer (International Light IL-1700 with SED-008 detector), calibrated against a NIST-traceable standard at each of the peak wavelengths indicated in Table 1. Following UV exposure, coupons were returned to SafeTraces laboratories (Pleasanton, California) in light-protective bags for DNA quantification by ddPCR.

2.3. Bacteriophage liquid suspension

Pure strains of the MS2 bacteriophage (ATCC 15597-B1) and its host bacterium (*E. coli* ATCC 15597) were obtained from ATCC by ARE Laboratory (Aerosol Research and Engineering Laboratories, Inc.) at Overland Park, Kansas City, USA. To culture MS2, liquid media was inoculated with the bacteriophage during the logarithmic growth phase of the host bacteria. After an appropriate incubation period (37 °C, overnight 16 h ± 2 h), cells were lysed, and cellular debris separated by centrifugation. MS2 yields were greater than 10^{11} plaque forming units (pfu) per mL with a single amplification procedure. The stock suspension was then diluted with phosphate buffered saline (PBS, Bioland Scientific LLC; Cat: PBS01-03) to a target of 10^{10} pfu/mL, before it was used to generate MS2-tagged aerosols with a pneumatic nebulizer (SafeTraces, Inc., model ES-1 eSprayer).

2.4. Aerosol generation device

The device works with a pressurized air tank at 448.2 kPa, connected by a line to a liquid reservoir and a spray nozzle. The liquid reservoir contains the target tracer at a known concentration. The DNA-tagged liquid suspension and the bacteriophage liquid suspension were sprayed independently and simultaneously using the same model of pneumatic nebulizers (SafeTraces, Inc.). The device is capable of aerosolizing 5 mL of liquid suspension in 4 s. The particle size distribution generated by this pneumatic nebulizer using a similar DNA tracer solution was measured with a laser diffraction instrument (Spraytec, Malvern Panalytical Ltd.), placed 0.15 m from the nebulizer nozzle, the volumetric median particle size was 24.05 ± 0.25 μm (SD from triplicate) with 10th and 90th percentiles of 6.96 and 79.23 μm, respectively [12].

Table 1
UVGI fixture lamp types used for UVGI fixture exposure with collimated beams.

UV Lamp Type	Nominal Peak Wavelength (nm)	Manufacturer and Model Number	Company Location
Krypton Chloride excimer (KrCl), optically-filtered	222	Ushio America, Inc. Model B1	Cypress, California, USA.
Low-pressure mercury (non-ozone producing)	254	Aquafine Model 9135-L61	Valencia, California, USA.
UV Light Emitting Diode (UV LED)	282	Nichia Corporation Model NCSU434C	Tokushima, Japan.

2.5. Aerosolization of DNA-tagged and bacteriophage suspensions in test chamber

To test sensitivity to UV radiation, liquid suspensions were aerosolized within a 1050 cubic feet (30 m^3) test chamber with both DNA-Tagged and MS2 bacteriophage. Four UVGI fixtures were used for UV exposure (Table 2, see Table S1 for device power), Aeromed Lexus 2.1 is an upper room UVGI device at 254 nm; Far UV Krypton is a whole room irradiation device at 222 nm wavelength [18–20] that is optically filtered from 200 to 230 nm; Bolb SUVOS-25 is an LED device for unoccupied space disinfection at 275 nm wavelength; and the AuraBlue AB24 is an air troffer with enclosed 275 nm UV LEDs, with an internal fan that was run at 160 CFM (271.8 m^3/h), low power mode, but could be run at a flow rate as high as 430.3 CFM (731 m^3/h).

A control condition with no UV device was included to assess natural aerosol decay. The UV devices were placed in the chamber successively, oriented to the center of the room, and removed before the next device was tested. At least three independent replicates of aerosol release, exposure to UV from the device for 1 h, and sample collection were performed. An Optical Particle Sizer (OPS) (TSI, Inc., model 3330) was used to monitor the aerosolized particle size distribution, which was supported by monitoring the total particle concentration. Between experimental replicates, the air from the chamber was purged through HEPA-filters to outdoor air between 15 and 20 min until particle concentrations reached background levels confirmed by the OPS in real time.

Inside the test chamber, the simultaneous aerosolization of 5 mL DNA-tagged tracer and 5 mL bacteriophage MS2 in PBS and Tryptic soy broth (Neogen, Cat: NCM0004A) were performed using two separate pneumatic nebulizers to prevent potential mixing interactions that could interfere with DNA-tag sensitivity. The test chamber setup is shown in Fig. 1. Two mixing fans located as shown and inclined 45° upward from the horizontal plane were operated during the initial 5 min post-aerosolization to promote mixing. Fan specifications included Mixing fan 1 (Amazon, model fanmk01) providing 197 CFM (334.7 m^3/h), Mixing fan 2 (Honeywell, model HTF1220B) producing a flow of 478 CFM (812.1 m^3/h), and one ceiling fan (4.5 ft diameter) maintaining continuous airflow at 613 CFM (1041.5 m^3/h). Temperature and relative humidity were monitored throughout all experiments (AC infinity, model Controller 69), with ranges of 17.8–24.4 °C and 39%–50 % RH, respectively (with a maximum change of 1.1 °C and 1 % RH within replicates).

2.6. Air sampling

DNA-tagged aerosols were sampled with an automatic air sampling system (SafeTraces, Inc., model AS-4 AutoSampler). The system consisted of four devices; each one capable of collecting four sequential air filter samples given a defined sampling interval duration (Fig. 2). The system was equipped with a pump calibrated at 5.5 ± 0.1 L/min, and the air passed through a 25 mm glass microfiber filter with a 1.0 μm nominal pore size (grade A-E, Sterlitech Corp.). This allowed for precise and controlled sample collection, ensuring the retrieval of airborne particles containing the DNA tracer. The filters were held inside a cassette (25 mm, clear styrene, SKC PN 225-2-25LF), and at the end of the programmed sampling period collected and sent to the laboratory (SafeTraces) for DNA quantification.

Table 2
UVGI fixture fixtures used in this study from various manufacturers.

Device	Light Source	Wavelength	UV Irradiance	Distance from Device	Radiometer Used
Lexus 2.1 Aeromed	Mercury Lamp	254 nm	260 μW/cm^2	1 m	General UV512C
Krypton Far UV	krypton-chloride	222 nm	13 μW/cm^2	0.48 m	Hopocolor Model 220UVGI fixture
SUVOS-25 Bolb	LED	275 nm	26 μW/cm^2	1 m	General UV512C
AB24 AuraBlue	LED	275 nm	[a]1200 μW/cm^2	430 mm from the LED inside device.	International Light ILT770-UV

[a] No UV Irradiance measured outside of the device.

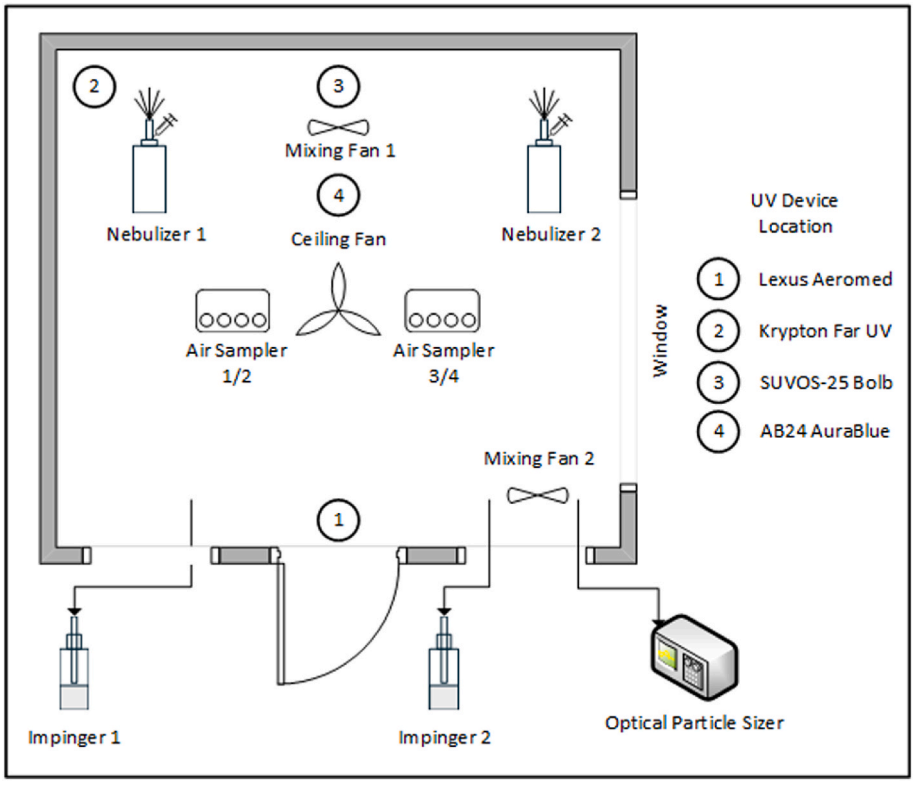

Fig. 1. Experimental chamber schematic.

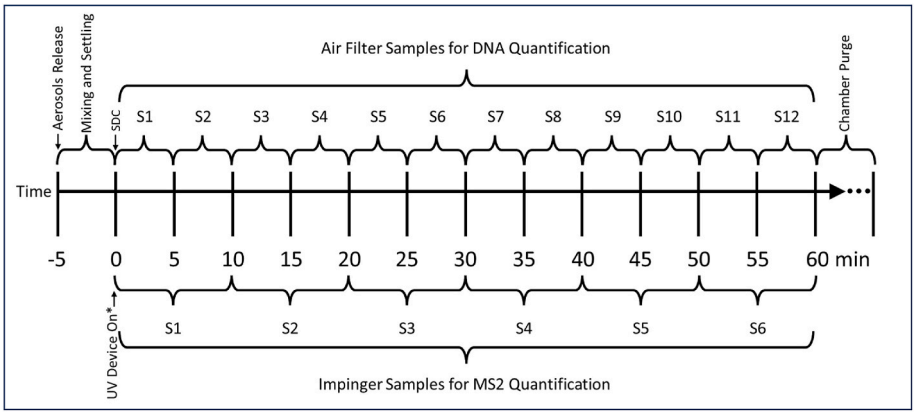

Fig. 2. Air sampling timeline. SDC: Start of Decay Curve. *SUVOS-25 Bolb Turned on at −5 min.

Additionally, two AGI-30 impingers were used to sample the air inside of the chamber for bacteriophage quantification. These impingers were connected to two ports on opposite ends of the chamber to obtain a representative air sample. The AGI-30 impingers were designed with a critical orifice that pulled at precisely 12.5 LPM when connected to a vacuum. These impingers impacted the aerosol into 20 mL of PBS with an addition of 0.005 % volume of Tween 80 (Sigma-Aldrich; Cat P4780). Each sample was collected for a period of 10 min to get a suspension of bacteriophage from the aerosols in the air. For each sampled interval, the two suspensions were mixed and sent to the laboratory (ARE) for quantification.

2.7. DNA tracer quantification

To elucidate the impact of UV exposure on the DNA tags, the highly sensitive quantitative ddPCR approach [21] was used. This technique allowed for the precise quantification of specific DNA sequences. ddPCR utilizes water-oil emulsion technology to fractionate the reaction volume into approximately 20,000 droplets. Each droplet underwent PCR amplification, which enabled the measurement of thousands of amplification events within a single reaction well.

The DNA tags from the foil coupons were extracted for subsequent analysis by washing with a proprietary aqueous buffer solution. Similarly, the Sterlitech 1-μm (AE2500) cassette filters integrated into SafeTraces air samplers were subjected to DNA extraction using the same buffer composition used for the foil coupons. The samples were diluted to an appropriate concentration to fall within the optimum range (0–5000 copies per μL) for the ddPCR system. The comprehensive sample processing and dilution steps were implemented to guarantee that the subsequent ddPCR analysis would yield reliable quantitative results, enabling a detailed assessment of the impact of UV exposure on the DNA tags under various experimental conditions.

The reagents utilized in the ddPCR amplification included ddPCR Supermix for Probes no dUTP [ddPCR Part Number: 1863025] and two TaqMan probe assays. Each TaqMan probe was unique to one sequence, enabling discrimination between the two targets by the use of distinct fluorophores. The TaqMan probe for the UV-resistant tag was labeled with the HEX fluorophore, while the TaqMan probe for the UV-sensitive tag was labeled with the FAM fluorophore. Each TaqMan probe was custom ordered and acquired from IDT.

To generate the droplets required for ddPCR, Droplet Generation Oil for Probes [ddPCR Part Number: 1863005], ddPCR 8-Well Cartridges [ddPCR Part Number: 1864008], ddPCR Gasket Seals for 8-Well Cartridges [ddPCR Part Number: 1863009], a DG8 Cartridge Holder, and a QX200™ Droplet Generator were used. The consumables required for ddPCR analysis consisted of ddPCR 96-well Plates [ddPCR Part Number: 12001925] and PCR Plate Heat Seals [ddPCR Part Number: 1814040]. To perform the ddPCR analysis a PX1 PCR™ Plate Sealer, a C1000 Touch™ Thermal Cycler, and a QX200™ Droplet Reader were utilized.

2.7.1. DNA-tracer quantification experimental protocol

Each diluted DNA sample, extracted from foil coupons and air sampler cassettes, was subjected to ddPCR analysis using the specified TaqMan probes. The amplification reactions were performed on a ddPCR thermal cycler, and the resulting droplets were analyzed using the QX200 Droplet Reader (for a list of reagents used in DNA analysis see Table S2, for details on the thermal cycling protocol see Table S3).

This method allowed for the quantification of both UV-sensitive and UV-insensitive tags, providing a robust means to assess the effectiveness of UV exposure in altering the DNA tags' integrity. The utilization of specific TaqMan probes and associated consumables ensured the accuracy and reliability of the ddPCR-based analysis.

2.8. Bacteriophage quantification

The liquid suspensions obtained from impingers sampling air from the chamber were serially diluted with PBS (containing Tween 80 as described in the section air sampling) and plated in triplicate. This was done using a standard drop plaque assay technique onto tryptic soy agar plates (Hardy Diagnostics) with its host (*E. coli*). Plates were incubated at 37 °C overnight (between 12 and 16 h) and the enumeration was recorded by quantifying the plaques formed on the plates [22]. Technical triplicate results from each sample were averaged, and the concentration in the sample suspension as pfu/mL was determined. This value was used to calculate the total pfu collected in the sample (based on the 20 mL collected), with this and the total volume of air sampled the calculation of the concentration as pfu per L of air was obtained.

2.9. Statistical analysis

All data organization, data cleaning, figures, and statistical analysis were performed with R version 4.0.3 and packages contained in the Tidyverse [23,24]. For coupons, the total DNA copies quantified per sample were transformed to Log base 10, and this value was used as the dependent variable in a linear regression model [25] with dose as the independent variable. For liquid aerosols containing DNA-tags or MS2 bacteriophage, quantified results as concentration in units of DNA copies per L of air, or pfu per L of air were used to calculate their decay rate, which was assumed to be a first-order process. Within experimental replicates, each value was standardized by calculating the natural log of the ratio of concentration after a given exposure period to the initial concentration observed in the same experimental replicate of aerosol emission and sampling:

$$\text{Aerosol Tag Reduction} = \text{Ln}(C_i/C_0) \quad \text{Eq. 1}$$

where:

Aerosol Tag Reduction = the normalized natural log reduction of the DNA-Tag or MS2 bacteriophage concentration.

C_i = concentration at time i.

C_0 = initial concentration as a reference point, defined as time 0 min from aerosols decay.

The aerosol tag reduction values were transformed to positive magnitude and used as the dependent variable in a regression model using time as the independent variable. The initial time (time = zero) was defined as 5 min after aerosols release to provide enough time for aerosols to mix in the air and a stable log-linear decay rate measurement. This point is called the "Start of the Decay Curve'' (SDC), similar to how it is described in Appendix C of the ASHRAE standard 241 [26]. An exception was made for the SUVOS-25 Bolb device, for which the SDC was defined to be 10 min after aerosols were released, given that when observing the data, it was noted that more time was needed to have a log-linear decay for this device setting for the bacteriophage MS2. This exception was necessary, because the SUVOS-25 Bolb device had to be on during the initial air mixing period of 5 min with mixing fans on, albeit it was rigged with a flap to cover the UV LEDs, which was triggered to drop after the 5 min. This was not the case for the other three devices tested, which were turned on remotely after 5 min of air mixing. We believe that even though the flap was to prevent early exposure to UV from SUVOS-25, there was some aerosol being affected by UV behind the flap in the aerosol mixing period, which may have contributed to some signal instability during that time. The SUVOS-25 Bolb device is not intended for occupied spaces. Air mixing is important for reaching equilibrium of the aerosol and is allowed in testing according to the ASHRAE 241 standard. One model slope was obtained for each aerosol tag (MS2, Tag-D1, Tag-LM4) and device condition (UVGI off as control, plus 4 devices) combination (total = 15). The slope of the decay rate was interpreted as the equivalent air changes per hour (eACH), similar to how air changes per hour are calculated in the ASTM Method E741-11 (Eq. (2) below), which is used for measuring the air change rate in a room with outdoor air by means of a tracer gas [27].

$$Y = aX + b \quad \text{Eq. 2}$$

where:

Y = - Aerosol Tag Reduction (Eq. (1)).

a = slope, interpreted as eACH.

X = time since Start of Decay Curve in hours.

b = Y value when time equals zero (intercept).

For all the models, a significance level of 5 % was used to reject the null hypothesis of no reduction given increased time (or dose) of exposure to UV.

The effectiveness of each UVGI device was also calculated in the form of equivalent clean airflow delivery rate as described in Appendix A of the ASHRAE standard 241 for getting a better understanding on

scalability of the results. The equation is shown below (Eq. (3)):

$$V_{ACS} = V^*(K_{td} - K_{nd}) \quad \text{Eq. 3}$$

where:

V_{ACS} = air cleaning system equivalent clean airflow rate, CFM.

V = test chamber volume, ft^3.

K_{td} = infectious microorganism (MS2) decay rate with air cleaning system operating, $minute^{-1}$.

K_{nd} = infectious microorganism (MS2) decay rate without air cleaning system operating, $minute^{-1}$.

3. Results

3.1. UV sensitivity on surfaces

The results of the UV exposure experiments on foil coupons, focusing on the UV-sensitive and resistant tags, are presented in Fig. 3. The investigation covered UV wavelengths of 222 nm, 254 nm, and 282 nm, with doses ranging from 0 to 100 mJ/cm^2. The y-axis represents the total DNA copies measured using ddPCR, while the x-axis plots the dose in mJ/cm^2.

Table S4 summarizes results used to create a linear model of DNA-tag decay based on the dose applied on coupon surfaces. Doses of UV at the three wavelengths tested ranged from 0 to 100 mJ/cm^2 for DNA-tagged tracer D1 and 0–50 mJ/cm^2 for DNA-tagged tracer LM4 in the linear range of response for tracer decay (see Fig. 3). A total of 14–18 observations were made for each of the data sets in Table S4, the range of copies of DNA quantified from the extraction of the coupons is reported from a minimum of $187.5x10^6$ DNA copies and maximum of $91.6x10^9$ DNA copies.

Distinct patterns were revealed in the UV dose response of the UV-sensitive tag (Tag-LM4, triangles on Fig. 3) at each wavelength. At 222 nm, a linear dose response was observed over the entire range of doses up to 100 mJ/cm^2, showing a reduction in DNA copies with increasing UV dose. For 254 nm and 282 nm, the UV-sensitive tag demonstrated a linear response up to 50 mJ/cm^2, beyond which the reduction in signal became non-linear (gray triangles, removed for statistical analysis). For Tag-LM4 using 222 nm, one observation at 100 mJ/cm^2 was noted to be highly influential with a Cooks' distance of 1.24. It was therefore removed from the analysis before model estimations [25,28]. Separately, in the case of Tag-LM4 and the wavelength 254 nm and 282 nm, the group of values removed was because their presence showed a non-linear trend (lack of fit due to no random errors) in the residuals values when plotted against dose as the independent variable, or subsequently showed high influence in the decay rate estimations. For Tag-LM4 and the wavelengths 222 nm, 254 nm, 282 nm the coefficient of determination (r^2) was improved to 88 %, 92 %, and 98 % respectively from 80 %, 87 %, and 59 % when the points that did not fit well with the log-linear models were removed. Notably, the UV-resistant tag exhibited substantially less reduction in signal across all UV wavelengths and doses (red dots and lines, Tag-D1), indicating its resistance to the effects of UV exposure. The foil coupons exhibit large changes with the dose exposures, and it should be noted that the coupons were hand spotted and air-dried, which can contribute to some noise in the data.

Table 3 includes exponential rates of decay, obtained from simple linear regression of the log-transformed variable DNA copies. Decay rates were estimated between 0 and 50 mJ/cm^2 for Tag-LM4, and between 0 and 100 mJ/cm^2 for Tag-D1. The UV dose (mJ/cm^2) per 1 Log_{10} reduction of MS2 (Phage) ATCC 15597 is reported in the literature around 19–20 mJ/cm^2 (Table 4) [29]. For reference, a 254 nm UVC dose of 20.06 mJ/cm2 has shown potential for more than 4 Log_{10} reduction of other pathogens like SARS-CoV-2 [30,31]. DNA-tag LM4 is close to the reported bacteriophage MS2 with a dose ranging between 24.0 and 78.1 mJ/cm^2 for 1 Log_{10} reduction in the range of wavelengths tested. DNA-tag D1 requires at least one order of magnitude of more dose to be equivalent in response to the bacteriophage MS2, which is why it is considered more resistant to UV than DNA-tag LM4. These findings underscore the differential impact, detected by the DNA-tagged tracers, of UV exposure and UV-induced DNA damage.

The observed reduction in DNA copies on a UV dose basis highlights the efficacy of UV in diminishing the amplifiable DNA content, establishing a relationship between DNA UV-induced damage assessment and its potential application in UV-exposed environments.

3.2. UV sensitivity of DNA-tagged aerosols and MS2 bacteriophage

As expected, the bacteriophage MS2 sensitivity to UVGI showed a great range of variation, with reduction differences of orders of magnitude among devices. A summary of the range of values observed is presented in Table S5. The highest reduction in concentration for an individual sample was observed in the Lexus 2.1 device (Table S5). However, in terms of rate (Table 5), the SUVOS-25 showed a higher sensitivity than the Lexus 2.1, with estimated values of 9.97 eACH and 9.27 eACH, respectively. The AB24 and Krypton devices followed with decay rates equivalent to 5.48 eACH and 2.30 eACH, respectively. When the UVGI devices were used, all estimated decay rates were on average higher than the natural decay observed in the chamber, which was estimated at 1.53 eACH (Fig. 4).

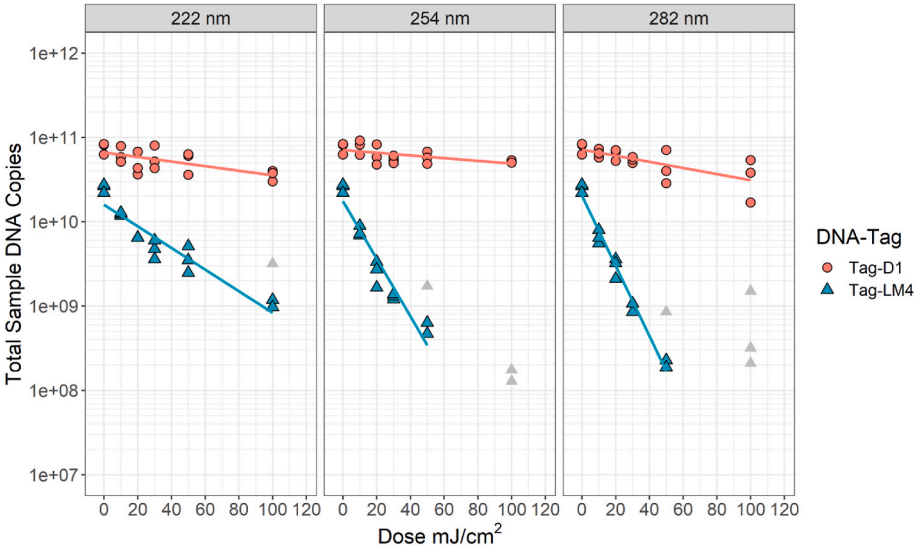

Fig. 3. UV Exposure effects on DNA-Tracer tags on the surface of coupons.

Table 3
The decay rates as a function of UV irradiance at wavelengths 222 nm, 254 nm, and 282 nm with respect to UV-resistant Tag-D1 and UV-sensitive Tag-LM4 dried on foil coupons.

DNA-Tag	Wavelength nm	Estimate	Std. Error	Statistic	*p-value*	95 %C.I.	
						$Log_{10}DNAcopies/(mJ/cm^2)$	
		$Log_{10}DNAcopies/(mJ/cm^2)$				Low	High
Tag-D1	222	−0.0027	0.0008	−3.54	0.003	−0.0043	−0.0011
	254	−0.0016	0.0006	−2.90	0.010	−0.0028	−0.0004
	282	−0.0036	0.0009	−4.08	0.001	−0.0055	−0.0017
Tag-LM4	222	−0.0128	0.0012	−10.38	<0.001	−0.0154	−0.0102
	254	−0.0342	0.0028	−12.06	<0.001	−0.0403	−0.0280
	282	−0.0416	0.0017	−24.10	<0.001	−0.0453	−0.0378

Table 4
UV Dose (mJ/cm^2) per 1 Log_{10} reduction of indicator/DNA-Tagged tracer.

Indicator/DNA-Tag	UV Dose (mJ/cm^2) for 1 Log_{10} reduction at different Wavelength		
	222 nm	254 nm	282 nm
Tag-D1	370.4	625.0	277.8
Tag-LM4	78.1	29.2	24.0
Bacteriophage MS2[a]	–	19 to 20	–

[a] MS2 value taken from Ref. [29].

For the DNA-tagged aerosol tracers, the results of UV inactivation are shown in Figs. 5 and 6. The maximum observed reduction for an individual sample was -2.40 $Ln(C/C_0)$ and -4.02 $Ln(C/C_0)$ for Tag-D1 and Tag-LM4 respectively (Table S6), both happening for exposure to the device SUVOS-25. There was a clear increase in the estimated eACH given the presence of the UVGI devices (Table 6), and as expected, Tag-LM4 showed higher decay rate with more sensitivity than Tag-D1. It is important to note that for Tag-LM4 when using SUVOS-25 the results followed a log-linear trend for 25 min. After this period, the values did not follow the same rate of reduction and were therefore omitted from the analysis.

Table 5
MS2 Bacteriophage decay in chamber models as eACH.

Aerosol Tag	UVGI Device Status	Estimate	Std. Error	Statistic	*p-value*	95 % C.I.		V_{ACS}
						Low	High	
		eACH				eACH	eACH	CFM
MS2 Bacteriophage	Device Off	1.53	0.18	8.38	<0.001	1.15	1.90	–
	Lexus Aeromed On	9.27	0.31	30.09	<0.001	8.62	9.92	134.85
	Krypton Far UV On	2.30	0.21	10.78	<0.001	1.85	2.75	13.48
	SUVOS-25 Bolb On	9.97	0.64	15.62	<0.001	8.59	11.35	146.98
	AB24 AuraBlue On	5.48	0.27	20.34	<0.001	4.91	6.05	68.82

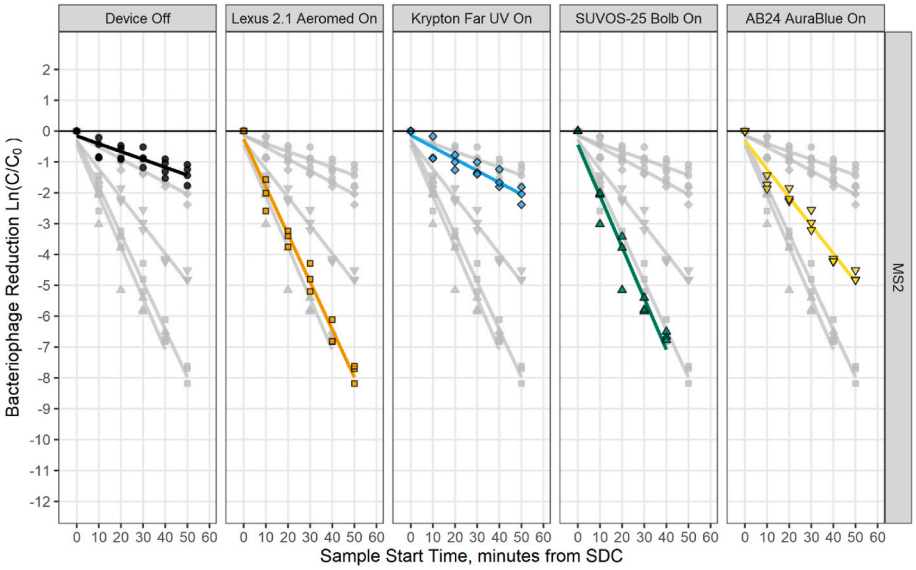

Fig. 4. UV Inactivation curves in logarithmic scale for aerosolized MS2 bacteriophage in a 30 m^3 sealed chamber. Solid colors represent the UV device condition values inside each facet, gray shaded values inside each facet represent the rest of the data for relative comparison. (For interpretation of the references to color in this figure legend, the reader is referred to the Web version of this article.)

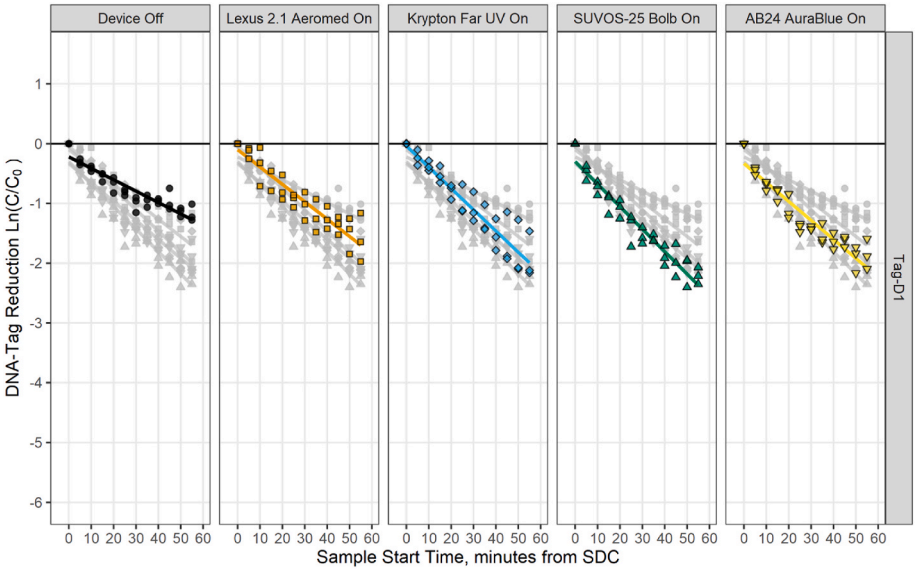

Fig. 5. UV Inactivation curves in logarithmic scale for aerosolized DNA Tag-D1 in a 30 m^3 sealed chamber.

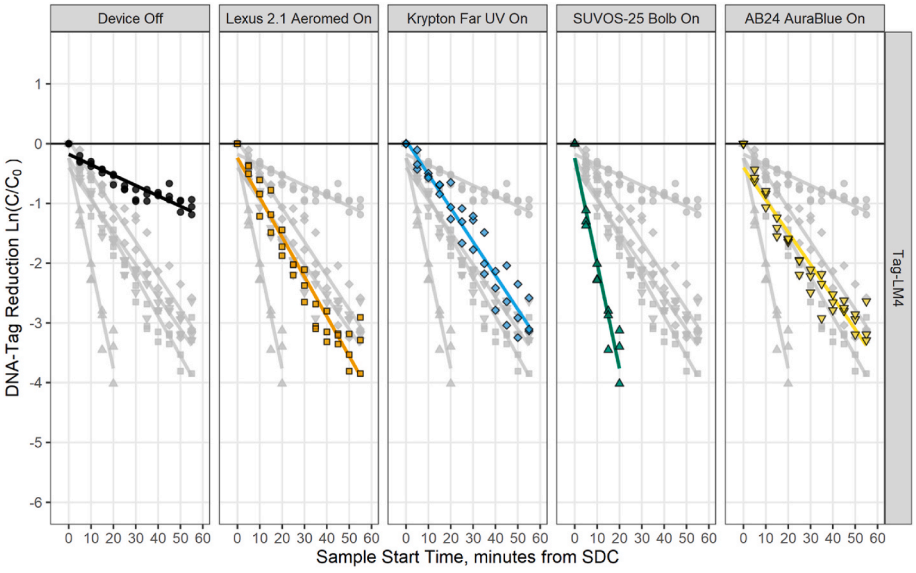

Fig. 6. UV Inactivation curves in logarithmic scale for aerosolized DNA Tag-LM4 in a 30 m^3 sealed chamber.

Table 6
DNA Tracer decay in chamber modeled as eACH.

Aerosol Tag	UVGI Device Status	Estimate	Std. Error	Statistic	*p-value*	95 % C.I.	
		eACH				Low	High
						eACH	eACH
Tag-D1	Device Off	1.14	0.08	14.03	<0.001	0.98	1.31
	Lexus Aeromed On	1.74	0.13	13.90	<0.001	1.49	2.00
	Krypton Far UV On	2.13	0.13	15.93	<0.001	1.86	2.41
	SUVOS-25 Bolb On	2.26	0.11	19.69	<0.001	2.02	2.49
	AB24 AuraBlue On	1.90	0.12	16.31	<0.001	1.67	2.14
Tag-LM4	Device Off	1.04	0.07	14.44	<0.001	0.90	1.19
	Lexus Aeromed On	3.99	0.19	21.32	<0.001	3.61	4.37
	Krypton Far UV On	3.39	0.16	20.92	<0.001	3.06	3.72
	SUVOS-25 Bolb On	10.57[a]	0.71	14.93	<0.001	9.04	12.10
	AB24 AuraBlue On	3.25	0.16	20.47	<0.001	2.93	3.57

[a] Log-linear relationship for model observed only up to 25 min after the start of aerosols decay.

3.2.1. Scaling factor

Using the linear regression estimates of eACH for each DNA-tag and the MS2 bacteriophage a relationship between their decay magnitudes was calculated (Table 7). The relationship shown in the following table can be used to estimate the bacteriophage reduction when only the DNA-tag decay rate is measured in a space.

3.3. Commercial building application of DNA-tracer tag

To assess the sensitivity of the DNA-tagged tracers under different UVGI fixture conditions in a commercial building setting, experiments were conducted in a conference room (Fig. 7). The dimensions of the room were 4.87 m by 4.57 m and floor to ceiling height 2.74 m, resulting in a volume of 61.16 m^3 (2160 ft^3). A square ceiling diffuser supplies roughly 42 L/s of air to the space, which is exhausted via a ceiling return grill diagonally opposite the supply, as shown in Fig. 7. The supply air flow rate corresponds to an air change rate of approximately 2.5 ACH. The return vented directly into the ceiling and a portion of the air likely was picked up again at some point in the system for recirculation, the exact amount is unknown. The baseline condition, with UVGI fixtures off, provided a reference point for comparison and to determine natural loss. Subsequent experiments involved testing each UVGI fixture individually, with the tracer aerosolized in the room. The Aeromed Lexus 2.1, Far-UV Krypton, and Bolb SUVOS-25 fixtures were placed near the corner of the room at a 45° angle from the uppermost wall in Fig. 7 to irradiate the largest volume of the room possible. The AuraBlue AB24 fixture was mounted in the drop ceiling of the conference room. Placement was limited by lights, fire sprinklers, ventilation ducts, and electrical cords within the drop ceiling. The deviation in placement for this fixture is deemed acceptable due to the mode of action used by the device. Air is pulled into the device where it passes through an enclosed chamber irradiated by the UVC LEDs, after which the air is returned to the room. The results, depicted in Figs. 8 and 9, illustrate the tracer's responsiveness to the diverse UVGI devices employed in the study. The varying levels of sensitivity observed in response to individual UVGI fixtures highlight the nuanced interactions between the tracer and different UV technologies, offering insights into the performance of these fixtures in commercial building indoor environments (Table S7 and Table 8).

4. Discussion

The study aimed to assess the feasibility of using DNA-tagged aerosol tracer particles for in situ testing in commercial buildings, allowing for the differentiation of UVGI fixture contributions to bioaerosol inactivation. These tracers, exemplified by the UV-sensitive LM4, proved effective in occupied spaces, and could scale with known airborne viral pathogen surrogates like MS2 bacteriophage. Several limitations of this study should be noted. One is the inability to aerosolize MS2 bacteriophage in the conference room setting, due to the impracticality of viral release in occupied spaces, another is the weak responsiveness of MS2 bacteriophage to 222 nm UVGI fixtures, also DNA does not address viral protein damage, and MS2 is a non-enveloped virus, so it will be a future study to evaluate if this is significant in the approach taken. Given the linear response of the DNA-tracer to UVGI, there should not be a great dependency of the scaling factor on the mechanism of UVGI inactivation, so long as all UVGI pathogen inactivation mechanisms behave log-linearly, irrespective of the specific type of damage. A future laboratory validation is recommended to observe the trend of decay between the various pathogens (i.e., enveloped vs. non-enveloped) and the DNA tracer. In our proposed methodology, sampling for 60 min is reliable for up to approximately 12 eACH, which is similar to the ASHRAE standard 241 [26]. Higher ventilation rates will reduce the signal too quickly and there will not be enough DNA signal to quantify the decay reliably above this threshold. From a practical point of view, the study demonstrated strong support for scaling and implementation in field testing. Furthermore, while DNA-tagged tracers currently model DNA damage only, they showed promising responsiveness to a broad range of UV-C wavelengths, including 222 nm wavelength exposure, suggesting potential for future testing with more susceptible viral surrogates sensitive to Far UV-C wavelengths and protein damage.

The implementation of a DNA-tracer-based approach, as demonstrated in this study, offers a tool for evaluating and optimizing indoor air quality in commercial building settings by providing a way to measure liquid aerosols reduction by ventilation, and UVGI contributions in units of equivalent ventilation (as V_{ACS}) as shown in Table 9. The UV-sensitive tracers, when aerosolized in conjunction with the MS2 phage under controlled test chamber conditions, provide an understanding of the dynamics of these surrogate airborne particles under ideal test conditions: zero air changes per hour, well mixed chamber via mixing fans, and allowing time for the aerosols to reach homogeneity. This controlled testing enabled scaling of the log reductions between the bacteriophage and the DNA-tagged tracers when exposed to UVGI fixture wavelengths. This scaling permits an assessment of the contributions of UVGI fixtures to the sampling points under study and correlates the DNA-tagged tracer data to MS2 bacteriophage UV inactivation behavior. This is possible because the controlled test chamber experiments under ideal conditions demonstrated high reproducibility, and because of the log linear trend of bacteriophage MS2 and DNA-tagged tracer decay rates. This was true for the UV off conditions as well as the UV on. Importantly, in the UV off condition, the MS2 bacteriophage and the DNA-tagged tracers' decay rates in the test chamber are similar, which is attributable to the matching of the chemical properties of the solutions for the bacteriophage and the DNA-tagged tracer. This allowed for similar particle sizes generated from the pneumatic nebulizers. The composition of the DNA-tagged tracers has been developed to mimic the chemical composition of human upper respiratory excretions. The same pneumatic nebulizers were used in the commercial conference room testing as the controlled test chamber, and thus provide confidence in correlating the results from the DNA-tagged tracers aerosolized in the

Table 7
Scaling factors for DNA-tracer decay to bacteriophage MS2 decay.

Aerosol Tag	UVGI Device	Device effect $\Delta = eACH_{UV\ On} - eACH_{UV\ Off}$		Decay Relationship ΔMS2/ΔDNA-Tag
		ΔMS2	ΔDNA-Tag	
Tag-D1	Lexus Aeromed On	7.74	0.60	12.91
	Krypton Far UV On	0.77	0.99	0.78
	SUVOS-25 Bolb On	8.44	1.11	7.59
	AB24 AuraBlue On	3.95	0.76	5.20
Tag-LM4	Lexus Aeromed On	7.74	2.94	2.63
	Krypton Far UV On	0.77	2.35	0.33
	SUVOS-25 Bolb On	8.44	9.53	0.89
	AB24 AuraBlue On	3.95	2.21	1.79

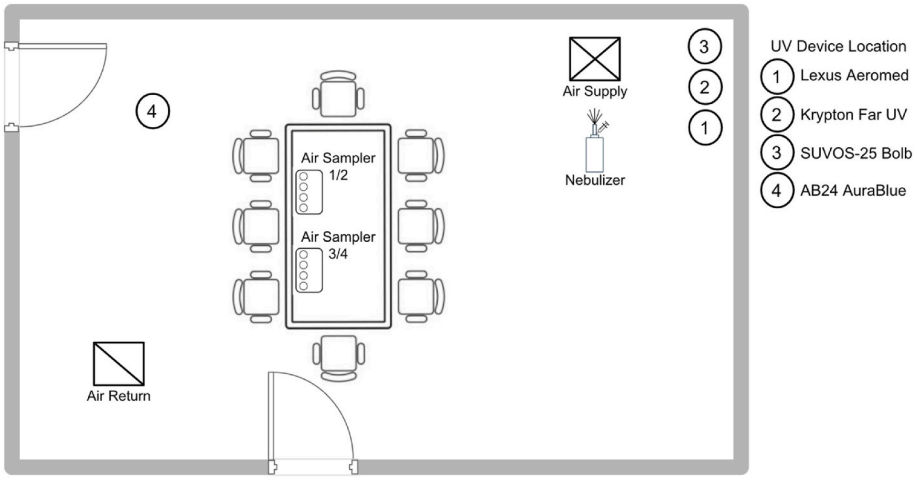

Fig. 7. UVGI configuration at a commercial conference room for effectiveness evaluation. Room size approximately 61.16 m^3 (2160 ft^3) in volume, doors closed during testing period, and the pneumatic nebulizer placed directly under the HVAC air supply. Air samplers were placed on the conference room table. The UVGI fixtures were located near the corner of the room at a 45° angle from the uppermost wall in the figure and were projecting UV towards the center of the room at various heights.

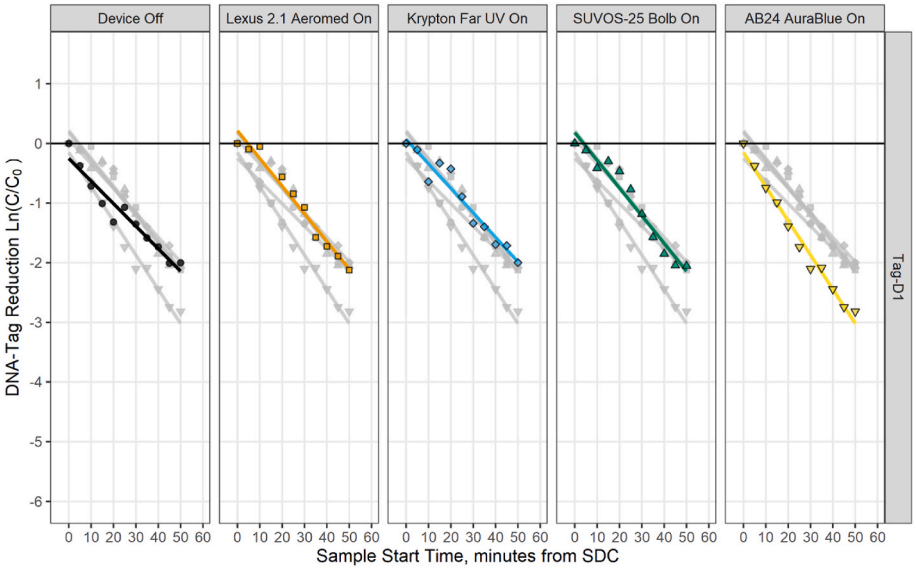

Fig. 8. UV Inactivation curves in logarithmic scale for aerosolized DNA Tag-D1 in a 61.16 m^3 conference room in a commercial building.

conference room with a scaling to MS2 bacteriophage, which we have consolidated in terms of eACH. A general limitation of in situ testing is that it is not easy to understand the air mixing behavior of the room under study. In situ scenarios are typically not well mixed due to unique geometries, occupancy, furniture, variable locations of HVAC supplies and returns, and other unique situational factors. By aerosolizing the DNA-tagged tracers and measuring the response from a selected origin point for aerosol emission, along with an informed selection of the location of the air samplers, it is possible to get a representative view of what is happening at the location of the air samplers. In the case of the conference room, the air samplers were placed on the conference room table, a position that has a high chance of being occupied in such a scenario. This technology gives a valuable snapshot of the airflow and UVGI dynamics at select, highly pertinent points in the building, and the ability to scale those results with how MS2 bacteriophage, a viral surrogate, would be expected to respond to ventilation, filtration, and any UVGI installed in that space.

4.1. Foil coupon testing

Our investigation commenced utilizing foil coupons with dried DNA-tagged tracers to elucidate the responses of the tracers to UV exposure at different wavelengths of UV radiation. This format permitted a streamlined workflow to assess UV dose response of the tracers tested. These experiments not only describe the wavelength-dependence of the intrinsic kinetics of the photochemical reactions that are responsible for DNA detection decay, but also inform the interpretation of data from testing of the effects of UVGI fixtures in actual use settings. The results of these experiments illustrated LM4's heightened sensitivity to 282 nm radiation, relative to radiation at shorter wavelengths, a phenomenon potentially influenced by DNA absorption characteristics. Importantly, LM4 is capable of detecting UV response across all three wavelengths tested. It is important to note also that the DNA-tagged tracers are synthetic DNA and are not encapsulated in a viral envelope or proteins. This is a limitation of the DNA tracer because UV damaging effects on proteins are not simulated by the DNA-tagged tracers, and only nucleic acid damage is simulated by the tracers. Nonetheless, the ability to

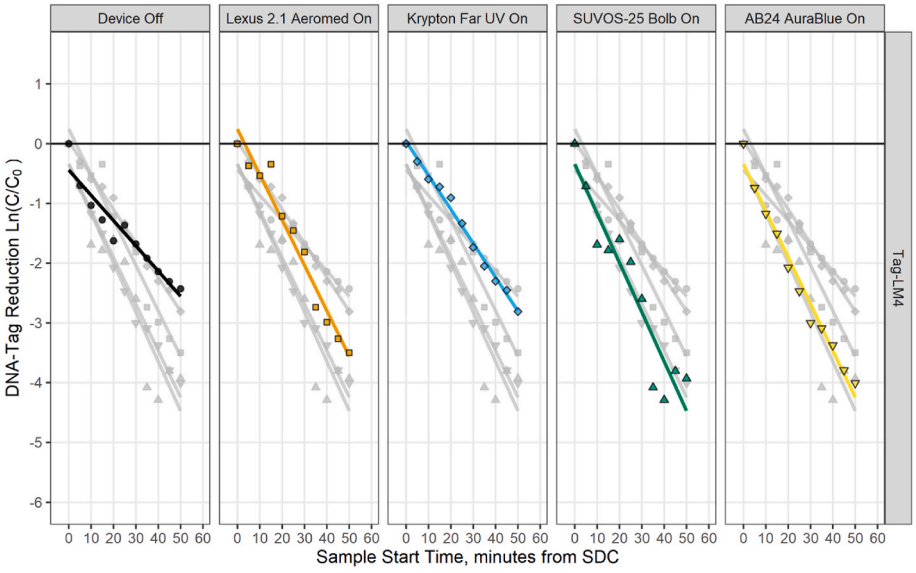

Fig. 9. UV Inactivation curves in logarithmic scale for aerosolized DNA Tag-LM4 in a 61.16 m^3 conference room in a commercial building.

Table 8
Summary of eACH for UVGI devices in DNA-tracer response to exposure in commercial office.

Aerosol Tag	UVGI Device Status	Estimate	Std. Error	Statistic	*p-value*	95 % C.I.	
		eACH				Low eACH	High eACH
Tag-D1	Device Off	2.27	0.19	11.96	<0.001	1.84	2.70
	Lexus Aeromed On	2.78	0.17	16.25	<0.001	2.39	3.18
	Krypton Far UV On	2.47	0.21	11.75	<0.001	1.99	2.94
	SUVOS-25 Bolb On	2.79	0.21	13.39	<0.001	2.32	3.26
	AB24 AuraBlue On	3.44	0.15	22.61	<0.001	3.10	3.79
Tag-LM4	Device Off	2.54	0.25	10.30	<0.001	1.98	3.09
	Lexus Aeromed On	4.56	0.31	14.66	<0.001	3.86	5.27
	Krypton Far UV On	3.41	0.11	31.53	<0.001	3.17	3.66
	SUVOS-25 Bolb On	4.95	0.58	8.55	<0.001	3.64	6.27
	AB24 AuraBlue On	4.69	0.23	20.78	<0.001	4.18	5.20

Table 9
Scaling of commercial building results with MS2 bacteriophage.

Aerosol Tag	UVGI Device	UV Off eACH	UV On eACH	Delta-Tag UV_{On-Off}	Decay Relationship ΔMS2/ΔDNA-Tag	ΔMS2 Estimation eACH	[a]V_{ACS} CFM	Total MS2 eACH
Tag-D1	Lexus Aeromed	2.27	2.78	0.52	12.91	6.65	239.40	8.92
	Krypton Far UV	2.27	2.47	0.20	0.78	0.16	5.76	2.43
	SUVOS-25 Bolb	2.27	2.79	0.52	7.59	3.95	142.20	6.22
	AB24 AuraBlue	2.27	3.44	1.17	5.20	6.10	219.60	8.37
Tag-LM4	Lexus Aeromed	2.54	4.56	2.03	2.63	5.33	191.88	7.87
	Krypton Far UV	2.54	3.41	0.88	0.33	0.29	10.44	2.83
	SUVOS-25 Bolb	2.54	4.95	2.42	0.89	2.14	77.04	4.68
	AB24 AuraBlue	2.54	4.69	2.15	1.79	3.85	138.60	6.38

[a] Calculated with a room volume of 61.16 m^3 (2160 ft^3). This is the air cleaning system equivalent clean airflow rate.

accurately quantify the effects of UV exposure through a safe, inert aerosol that can be used in occupied spaces provides insights into commercial building applications, heretofore, not possible with other technologies like radiometric readings and inert gas release studies. Future work in developing tracers may include estimating protein damage to the aerosol tracers. Another important finding with the UV-sensitive tracer, LM4, is that there is a point in the UV dose response behavior (at doses above 50 mJ/cm^2), where there is a non-linearity in LM4 response, not seen with tracer D1. This nonlinearity appears as a "hockey stick" shape, with a leveling out of the decay response at these

higher doses (Fig. 3). One possible explanation for this behavior is that the UV photodamage tracer LM4 has reached an equilibrium in the forward and reverse reaction of creation and undoing of photodamage, such as thymine dimer formation [32]. UV-induced photoproducts do not necessarily break the DNA backbone, and thus it is possible that at this energy regime, an equilibrium condition could develop. Only the linear portion of the dose response was considered in the subsequent analysis of the decay rates for LM4.

4.2. Aerosolized testing in a 30 cubic meter test chamber

Transitioning to aerosolized testing in a 30 cubic meter controlled test chamber at 0 ACH conditions, the effectiveness of the UV-sensitive DNA-tagged tracer LM4 in responding to UV doses at different UVGI fixture wavelengths from different devices was assessed. The UV-resistant DNA-tagged tracer D1, exhibits a smaller and less accurate change of response for UV on/off compared to LM4, as expected for a more UV-resistant DNA tracer. This difference underscores the benefit of LM4 being sensitive to UV exposure.

Despite challenges in measuring the Krypton 222 nm UVGI device's reduction response with aerosolized bacteriophage MS2 in the test chamber, DNA-tagged tracer LM4 aerosolized in the same test chamber is able to detect the effect of 222 nm exposure, as shown in Figs. 5 and 6. In this example of wavelength (222 nm) and DNA tracer Tag-LM4, it is interesting that the tracer outperforms the bacteriophage viral surrogate in sensitivity to UV doses in the Far UVGI fixture spectrum. Simultaneously releasing MS2 phage and aerosolized DNA-tracers Tag-D1 and Tag-LM4 in these tests, Figs. 4–6 underscore Tag-LM4's superior sensitivity to the UVGI fixture at 222 nm, in comparison to the MS2 bacteriophage's response, serving as a human viral pathogenic surrogate, in the Far UVGI fixture spectrum (222 nm). These results imply that bacteriophage MS2 may not be a good surrogate for Far UV germicidal fixtures. Bacteriophage MS2 was chosen in this study for the reason that it best fit the guidelines of standards such as the recently published ASHRAE Standard 241–2023 [26]. As there was no large change in bacteriophage MS2 with the 222 nm device, the scaling factor is probably not entirely reliable for this regime of UVGI fixture, and in future studies, a more sensitive, viral surrogate might be considered for demonstrating the efficacy of Far UV technology with our UV-sensitive DNA-tagged tracers. Ideal challenge agents will demonstrate UV dose-response behavior that is slightly conservative, as compared to target pathogens [33].

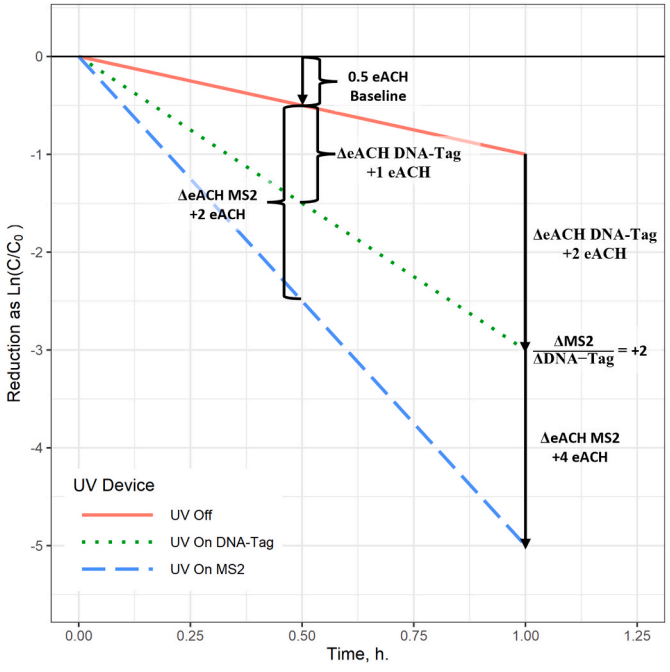

Fig. 10. Scaling factor for MS2 and DNA-Tag explanation.

It is important to note that the LED-based SUVOS-25 produced a powerful effect in the test chamber in terms of log reduction over time, as seen in Fig. 6 and Table 6 with tag LM-4, which was log-linear only within 25 min. After 25 min, the values did not follow the same reduction rate. There is a "hockey-stick" effect in the data after 25 min for SUVOS-25, similar to the "hockey-stick" non-linearity seen with Tag-LM4 at higher wavelengths and UV doses on foil coupon exposure (Fig. 3). This effect could imply and contribute to inaccuracy when scaling between surrogate bacteriophage and DNA-tagged tracers of very high powered UVGI devices. This is why we chose to scale only in the linear response range, the first 25 min, for Tag-LM4 with this device in the test chamber.

4.3. Comparison of scaled MS2 results in test chamber

A scaling factor, derived by converting logarithmic reductions to equivalent air changes per hour, facilitated the assessment of UVGI fixture efficacy. The scaling factor, calculated on a per-fixture basis, represents the ratio of the delta in eACH between UV off and on conditions for both the bacteriophage and the tracer. This approach provides an understanding of the impact of UVGI fixtures on the DNA tracers and a facile way to scale to a pathogen surrogate, in this case MS2 bacteriophage. Fig. 10 provides a quick view on how the scaling factor between MS2 and DNA-Tag is kept constant if it is calculated as reduction rates on eACH unit, which is a logarithmic scale. This implies that, if the eACH for the DNA-Tag is known, the eACH for MS2 can be calculated. It is important to highlight that this is only an accurate estimation if the decay rate of the DNA-Tag and MS2 are log-linear during the whole period of measurement, therefore, the data collected during experimentation should always be inspected for this assumption.

Table 7 outlines the scaling of the responses to the four UVGI fixtures and their UV exposures in the controlled test chamber of the DNA-tagged tracers scaled to the same UV exposures of bacteriophage MS2. Table 6 and Figs. 5 and 6 illustrate the response of both DNA-tagged tracers to exposure to UV light from the four test fixtures tested in the controlled aerosol test chamber. For Tag-D1, its resistance to UV-C decay significantly affects the accuracy of the scaling relationship, mathematically as the delta of the DNA-tagged tracer's response under UV on vs UV off conditions approaches zero, the scaling factor goes to infinity, emphasizing the unsuitability of Tag-D1 as a surrogate due to its greater variability and lower sensitivity, compared with DNA-tagged tracer Tag-LM4. While comparing the scaled MS2 results for Tag-LM4 and Tag-D1 in Table 9, the proximity of their outcomes shows that Tag-D1 results are potentially useful, but in most of the cases, given the high scale relationship they could end in higher equivalent reduction rates. For the previous reason, our study supports the idea that Tag-LM4 provides a more accurate representation, in addition to its wider range of measurement of change given its sensitivity.

4.4. Commercial building conference room testing

Expanding our investigation beyond controlled environments, experiments in a commercial building conference room demonstrate the adaptability of the DNA-tracer system. In the context of our findings, the differences between AB24 (a UVGI troffer fixture) in the commercial building application and controlled test chamber conditions were unexpected, with AB24 performing much better than SUVOS-25 in the commercial building setting. Comparing results from the chamber to the conference room, AB24 changed from a V_{ACS} of 68.82 CFM to 138.60 CFM (101 percent higher than in chamber), in contrast SUVOS-25 changed from 146.98 CFM to 77.04 CFM (47 percent lower than in chamber). This highlights the importance of validating results in practical settings. The unique airflow geometries of the conference room,

distinct from the continuous fans in the test chamber, likely contributed to these variations, as well as a troffer having its own fan at approximately 125 CFM (212.4 m^3/h). Another possibility is that the SUVOS-25 device might be better scaled with Tag-D1, as it was linear over the full hour in the test chamber with Tag-D1 vs Tag-LM4 (Figs. 5 and 6). If this is the case, then the SUVOS-25 eACH is probably more accurately 6.22 vs. 4.68 for Tag-D1 and Tag-LM4 respectively, scaling with bacteriophage MS2 (Table 9). The test chamber experimentation was designed to provide the most accurate effect of the tracers to UV exposure under controlled conditions, with exceptional mixing and 0 ACH by sealing the chamber. The conference room, by contrast, has its own unique geometry from the room design, HVAC supply and return positions, tables, chairs, and equipment. The conference room air sampler positions were chosen to be between the supply and return and situated on the conference room table, where people would most likely be seated at any given time while it is in use.

The same four UVGI fixtures used in the controlled chamber testing, were then applied to the conference room to assess the DNA-tagged tracers' responses to the fixtures' UV output over 1 h. Table 9 yielded the final conversion of the conference room results scaled to MS2 bacteriophage in this scenario. The baseline eACH for the room, as determined by the no UV condition with Tag-D1 and Tag-LM4, was 2.27 eACH and 2.54 eACH, respectively. All of the UVGI devices tested contributed to an increased eACH and when scaled to MS2 bacteriophage reduction, the total eACH of the room ranged from 2.83 to 7.87 eACH based on the MS2 scaling with Tag-LM4 tracer (Table 9). These were significant improvements to the conference room's overall eACH, when translating to percentages, three devices Lexus, SUVOS-25, and AB24 increased the estimated MS2 decay rate to more than 99 % reduction per hour (equivalent of 4.6 eACH total).

The air cleaning system equivalent clean airflow rate in CFM (V_{ACS}) was also calculated in Table 9, using equation (3) in the methods. This calculates, according to ASHRAE Standard 241, the amount of equivalent clean airflow rate, at the air sampler positions, that air cleaning systems, in this case UVGI fixtures, are producing. The amount of equivalent clean air delivered to the air sampler locations on the conference room table ranged from 10.44 to 191.88 CFM after being scaled to bacteriophage MS2 (with Tag-LM4). In the ASHRAE 241 Standard, the recommended Equivalent Clean Air delivered to the space per person (ECAi) is 30 CFM for an office type space. Using this metric, the fixtures are adding enough CFM of equivalent clean air, at the conference room table, for the equivalent of an additional, approximate 0.4 to 6.4 people to be at the table. It is important to note that this is after scaling the DNA tracer response to bacteriophage MS2. The Krypton 222 nm device is likely underrepresented here when scaling to bacteriophage MS2 in terms of its effectiveness (0.4 additional people at the table), since Far UV-C wavelengths likely should be scaled to more sensitive surrogate viruses. Nonetheless, the non-Far UV-C fixtures, when scaled to bacteriophage MS2, yield 2.6 (SUVOS-25), 4.6 (AB24), and 6.4 (Lexus 2.1) additional people to be at the conference room table based on the V_{ACS} calculations for DNA Tag-LM4 scaled to bacteriophage MS2. This is a significant improvement to the room occupancy capability.

4.5. Ventilation effectiveness, guidelines and standards

Aligning with recent CDC guidelines, advocating for a minimum of five air changes per hour (residing in the CDC Covid-19 guidelines), our study contributes a practical and quantitative means of evaluating devices that can provide equivalent ventilation effectiveness [34]. Correlating log reductions of the DNA tracer and MS2 phage with a scaling factor, as detailed in our findings, provides insights essential for establishing healthier indoor environments. Such a scaling to one known surrogate pathogen, in this study MS2 bacteriophage, could then be correlated, or scaled, to known log reductions of actual airborne pathogens of concern. These scalings could be built upon data of logarithmic reductions of airborne pathogens to UV exposure from published literature, such as Kowalski [10]. This information can aid in determining whether a space meets or exceeds the recommended air changes per hour. Our results represent the level of risk protection in terms of equivalent air changes per hour (eACH) and alternatively, equivalent clean airflow rate in CFM (V_{ACS}). This is the estimation of the same pathogen decay rate that can be provided by different mechanisms such as ventilation and filtration, now parsed out in this case as germicidal UV-light contributions to healthier indoor environments [35]. ASHRAE Standard 241 outlines comprehensive specifications for employing filtration and air cleaning systems to efficiently and economically attain the necessary clean airflow requirements in a safe and effective manner.

5. Conclusions

Our research introduces a practical method for measuring UV effectiveness and optimizing indoor air quality in diverse settings. The comprehensive results from controlled experiments and commercial building scenarios highlight the versatility and adaptability of our DNA-based tracer system. This system is chemically inert and considered non-hazardous, which enables UV testing at the site of installation, while occupied. Precise measurements can be made on UV-sensitive DNA-tagged tracers and their response to UVGI fixtures by employing the highly quantitative droplet digital PCR methodology. This methodology offers a nuanced in situ measurement of the impact of UVGI fixtures on airborne particles through scaling the results to viral surrogates like bacteriophage MS2. The correlation between log reductions of the DNA tracer and the MS2 bacteriophage, along with the scaling factor, provides a quantitative means of evaluating a room's unique ventilation and pathogen disinfection effectiveness. Comparison of the data from the conference room setting with chamber data taken under controlled test conditions supports the idea of the importance of making measurements at the site of installation of such germicidal ultraviolet fixtures, which can be influenced by situational factors such as air flow, ventilation, room geometry, and office furniture configurations.

Funding/Disclosures

This research project was funded by SafeTraces, Inc.

CRediT authorship contribution statement

Ilan Arvelo: Writing – review & editing, Writing – original draft, Visualization, Validation, Supervision, Methodology, Investigation, Formal analysis, Data curation, Conceptualization. **Ernest R. Blatchley:** Writing – review & editing, Writing – original draft, Validation, Resources, Methodology, Investigation. **William P. Bahnfleth:** Writing – review & editing, Validation. **Phil Arnold:** Writing – review & editing, Writing – original draft, Validation, Supervision, Resources, Project administration, Methodology, Conceptualization. **Ashley Fry:** Writing – review & editing, Writing – original draft, Visualization, Validation, Resources, Investigation, Data curation, Conceptualization. **Maria Topete:** Writing – original draft, Validation, Resources, Investigation. **Ling Zhou:** Writing – original draft, Resources. **William Palmer:** Writing – original draft, Resources. **Patrick J. Piper:** Writing – original draft, Resources, Investigation. **Jianping Zhang:** Writing – original draft, Resources. **W. Andrew Dexter:** Writing – original draft, Validation, Investigation, Data curation. **Nilson Palma:** Data curation, Conceptualization. **Nicholas J. Heredia:** Writing – review & editing, Writing – original draft, Validation, Supervision, Project administration, Methodology, Investigation, Conceptualization.

Declaration of competing interest

The authors declare the following financial interests/personal relationships which may be considered as potential competing interests:

Nicholas J. Heredia received financial support from SafeTraces, Inc.

funding this research project, with additional non-financial support of equipment, supplies, statistical analysis, travel, and writing assistance. William P. Bahnfleth and Ernest R. Blatchley III are private consultants for SafeTraces, Inc. William P. Bahnfleth is part of the Editorial Advisory Board Members of the journal Building and Environment.

Data availability

Data will be made available on request.

Acknowledgements

The authors acknowledge Carlos E. Carpio from the Department of Agricultural and Applied Economics of Texas Tech University, Lubbock, Texas, for his guidance in the data analysis process and the interpretation of results. We would also like to thank Ulrike Hodges for project management assistance. These acknowledgements do not mean a formal agreement with all the findings and statements made in this publication.

Appendix A. Supplementary data

Supplementary data to this article can be found online at https://doi.org/10.1016/j.buildenv.2024.111828.

References

[1] N.H.L. Leung, Transmissibility and transmission of respiratory viruses, Nat. Rev. Microbiol. 19 (2021), https://doi.org/10.1038/s41579-021-00535-6.
[2] B.F. Leo, C.Y. Lin, K. Markandan, L.H. Saw, M.S. Mohd Nadzir, K. Govindaraju, I. I. Shariffuddin, R. Sankara, Y.W. Tiong, H. Pakalapati, M. Khalid, An overview of SARS-CoV-2 transmission and engineering strategies to mitigate risk, J. Build. Eng. 73 (2023) 106737, https://doi.org/10.1016/j.jobe.2023.106737.
[3] E.A. Nardell, S.J. Bucher, P.W. Brickner, C. Wang, R.L. Vincent, K. Becan-McBride, M.A. James, M. Michael, J.D. Wright, Safety of upper-room ultraviolet germicidal air disinfection for room occupants: results from the Tuberculosis Ultraviolet Shelter Study, Public Health Rep 123 (2008) 52–60, https://doi.org/10.1177/003335490812300108.
[4] F. Ibrahim, E.Z. Samsudin, A.R. Ishak, J. Sathasivam, Hospital indoor air quality and its relationships with building design, building operation, and occupant-related factors: a mini-review, Front. Public Heal. 10 (2022), https://doi.org/10.3389/fpubh.2022.1067764.
[5] C.A. Gilkeson, C.J. Noakes, M.A.I. Khan, Computational fluid dynamics modelling and optimisation of an upper-room ultraviolet germicidal irradiation system in a naturally ventilated hospital ward, Indoor Built Environ. 23 (2014), https://doi.org/10.1177/1420326X14532933.
[6] A. Alani, I.E. Barton, M.J. Seymour, L.C. Wrobel, Application of Lagrangian particle transport model to tuberculosis (TB) bacteria UV dosing in a ventilated isolation room, Int. J. Environ. Health Res. 11 (2001) 219–228, https://doi.org/10.1080/09603120020047000.
[7] C.C. Wang, K.A. Prather, J. Sznitman, J.L. Jimenez, S.S. Lakdawala, Z. Tufekci, L. C. Marr, Airborne transmission of respiratory viruses, Science 80 (2021) 373, https://doi.org/10.1126/science.abd9149.
[8] G.R. Johnson, L. Morawska, Z.D. Ristovski, M. Hargreaves, K. Mengersen, C.Y. H. Chao, M.P. Wan, Y. Li, X. Xie, D. Katoshevski, S. Corbett, Modality of human expired aerosol size distributions, J. Aerosol Sci. 42 (2011) 839–851, https://doi.org/10.1016/j.jaerosci.2011.07.009.
[9] N. Clements, I. Arvelo, P. Arnold, N.J. Heredia, U.W. Hodges, S. Deresinski, P. W. Cook, K.A. Hamilton, Informing building strategies to reduce infectious aerosol transmission risk by integrating DNA aerosol tracers with quantitative microbial risk assessment, Environ. Sci. Technol. 57 (2023) 5771–5781, https://doi.org/10.1021/acs.est.2c08131.
[10] W. Kowalski, Ultraviolet germicidal irradiation handbook: UVGI for air and surface disinfection. https://doi.org/10.1007/978-3-642-01999-9, 2009.
[11] R.N. Harding, C.A. Hara, S.B. Hall, E.A. Vitalis, C.B. Thomas, A.D. Jones, J.A. Day, V.R. Tur-Rojas, T. Jorgensen, E. Herchert, R. Yoder, E.K. Wheeler, G.R. Farquar, Unique DNA-barcoded aerosol test particles for studying aerosol transport, Aerosol Sci. Technol. 50 (2016) 429–435, https://doi.org/10.1080/02786826.2016.1162903.
[12] I. Arvelo, F. Pagone, J. Persky, C.E. Carpio, P. Arnold, N. Clements, Decay rates of two tracer gases compared to DNA-tagged liquid aerosol tracer particles : impact of varying dilution rate and filtration, Build. Environ. 212 (2022) 108819, https://doi.org/10.1016/j.buildenv.2022.108819.
[13] M.G. Kemp, A. Sancar, DNA excision repair: where do all the dimers go? Cell Cycle 11 (2012) 2997–3002, https://doi.org/10.4161/cc.21126.
[14] L.H.F. Mullenders, A.-M. Hazekamp-van Dokkum, W.H.J. Kalle, H. Vrieling, M. Z. Zdzienicka, A.A. van Zeeland, UV-induced photolesions, their repair and mutations, Mutat. Res. Toxicol. 299 (1993) 271–276, https://doi.org/10.1016/0165-1218(93)90103-K.
[15] J.A. Sikorsky, D.A. Primerano, T.W. Fenger, J. Denvir, DNA damage reduces Taq DNA polymerase fidelity and PCR amplification efficiency, Biochem. Biophys. Res. Commun. 355 (2007) 431–437, https://doi.org/10.1016/j.bbrc.2007.01.169.
[16] M. Otaki, Y. Higashino, Y. Yamada, Experimental validation of determinants of UV sensitivity using synthetic DNA, J. Photochem. Photobiol., A 12 (2022) 100139, https://doi.org/10.1016/j.jpap.2022.100139.
[17] S. Lim, E.R. Blatchley, UV dose-response behavior of air-exposed microorganisms, J. Environ. Eng. 138 (2012) 780–785, https://doi.org/10.1061/(ASCE)EE.1943-7870.0000535.
[18] M. Buonanno, D. Welch, I. Shuryak, D.J. Brenner, Far-UVC light (222 nm) efficiently and safely inactivates airborne human coronaviruses, Sci. Rep. 10 (2020) 1–8, https://doi.org/10.1038/s41598-020-67211-2.
[19] D. Welch, M. Buonanno, V. Grilj, I. Shuryak, C. Crickmore, A.W. Bigelow, G. Randers-Pehrson, G.W. Johnson, D.J. Brenner, Far-UVC light: a new tool to control the spread of airborne-mediated microbial diseases, Sci. Rep. 8 (2018) 1–7, https://doi.org/10.1038/s41598-018-21058-w.
[20] E.R. Blatchley, D.J. Brenner, H. Claus, T.E. Cowan, K.G. Linden, Y. Liu, T. Mao, S. J. Park, P.J. Piper, R.M. Simons, D.H. Sliney, Far UV-C radiation: an emerging tool for pandemic control, Crit. Rev. Environ. Sci. Technol. 53 (2023) 733–753, https://doi.org/10.1080/10643389.2022.2084315.
[21] B.J. Hindson, K.D. Ness, D.A. Masquelier, P. Belgrader, N.J. Heredia, A. J. Makarewicz, I.J. Bright, M.Y. Lucero, A.L. Hiddessen, T.C. Legler, T.K. Kitano, M. R. Hodel, J.F. Petersen, P.W. Wyatt, E.R. Steenblock, P.H. Shah, L.J. Bousse, C. B. Troup, J.C. Mellen, D.K. Wittmann, N.G. Erndt, T.H. Cauley, R.T. Koehler, A. P. So, S. Dube, K.A. Rose, L. Montesclaros, S. Wang, D.P. Stumbo, S.P. Hodges, S. Romine, F.P. Milanovich, H.E. White, J.F. Regan, G.A. Karlin-Neumann, C. M. Hindson, S. Saxonov, B.W. Colston, High-throughput droplet digital PCR system for absolute quantitation of DNA copy number, Anal. Chem. 83 (2011) 8604–8610, https://doi.org/10.1021/ac202028g.
[22] A. Mazzocco, T.E. Waddell, E. Lingohr, R.P. Johnson, Enumeration of bacteriophages using the Small drop plaque assay system, 81–85, https://doi.org/10.1007/978-1-60327-164-6_9, 2009.
[23] R Core Team, R: A Language and Environment for Statistical Computing, 2020. https://www.r-project.org/.
[24] H. Wickham, M. Averick, J. Bryan, W. Chang, L. McGowan, R. François, G. Grolemund, A. Hayes, L. Henry, J. Hester, M. Kuhn, T. Pedersen, E. Miller, S. Bache, K. Müller, J. Ooms, D. Robinson, D. Seidel, V. Spinu, K. Takahashi, D. Vaughan, C. Wilke, K. Woo, H. Yutani, Welcome to the Tidyverse, J. Open Source Softw. 4 (2019) 1686, https://doi.org/10.21105/joss.01686.
[25] E.J. Dietz, W. Mendenhall, T. Sincich, A Second Course in Statistics: regression analysis, J. Am. Stat. Assoc. 92 (1997) 797, https://doi.org/10.2307/2965740.
[26] ASHRAE, Standard 241, Control of Infectious Aerosols, 2023.
[27] ASTM International, ASTM E741 - 11, Standard Test Method for Determining Air Change in a Single Zone by Means of a Tracer Gas Dilution, ASTM, West Conshohocken, 2017, 2017.
[28] The Pennsylvania State University, Applied Regression Analysis, Identifying influential data points. https://online.stat.psu.edu/stat462/node/173/, 2018. (Accessed 26 January 2024).
[29] G. Chevrefils, E. Caron, H. Wright, G. Sakamoto, UV dose required to achieve Incremental log inactivation of bacteria, Protozoa and viruses, 38–45, https://www.uvclight.co.uk/media/dosage_for_uvc.pdf, 2006. (Accessed 16 February 2024).
[30] C.P. Viana Martins, C.S.F. Xavier, L. Cobrado, Disinfection methods against SARS-CoV-2: a systematic review, J. Hosp. Infect. 119 (2022) 84–117, https://doi.org/10.1016/j.jhin.2021.07.014.
[31] A. Gidari, S. Sabbatini, S. Bastianelli, S. Pierucci, C. Busti, D. Bartolini, A. M. Stabile, C. Monari, F. Galli, M. Rende, G. Cruciani, D. Francisci, SARS-CoV-2 Survival on surfaces and the effect of UV-C light, Viruses 13 (2021) 2–9, https://doi.org/10.3390/v13030408.
[32] Y.K. Law, R.A. Forties, X. Liu, M.G. Poirier, B. Kohler, Sequence-dependent thymine dimer formation and photoreversal rates in double-stranded DNA, Photochem. Photobiol. Sci. 12 (2013) 1431–1439, https://doi.org/10.1039/c3pp50078k.
[33] E.R. Blatchley, in: Photochemical Reactors: Theory, Methods, and Applications of Ultraviolet Radiation, first ed., Wiley, Hoboken, 2023.
[34] Center for Disiase Control and Prevention, Ventilation in Buildings, 2023. https://www.cdc.gov/coronavirus/2019-ncov/community/ventilation.html#print. (Accessed 16 February 2024).
[35] E. Kujundzic, F. Matalkah, C.J. Howard, M. Hernandez, S.L. Miller, UV air Cleaners and upper-room air ultraviolet germicidal irradiation for controlling airborne bacteria and Fungal Spores, J. Occup. Environ. Hyg. 3 (2006) 536–546, https://doi.org/10.1080/15459620600909799.